

# Peeling off effects in vertically-aligned Fe<sub>3</sub>C filled carbon nanotubes films grown by pyrolysis of ferrocene

Filippo S. Boi<sup>+, 1, 2, a)</sup> Daniel Medranda<sup>+, 1, 2</sup> Sameera Ivaturi<sup>1, 2</sup> Jiayu Wang,<sup>1</sup> Jian Guo,<sup>1</sup> Mu Lan,<sup>1</sup> Jiqiu Wen,<sup>3</sup> Shanling Wang,<sup>3</sup> Yi He,<sup>3</sup> Gavin Mountjoy,<sup>4</sup> Maureen A.C. Willis,<sup>1, 2, b)</sup> and Gang Xiang<sup>1, c)</sup>

<sup>1)</sup> College of Physical Science and Technology, Sichuan University, 610064, Chengdu, China

<sup>2)</sup> Sino-British Joint Materials Research Institute, Sichuan University, Chengdu 610064, China

<sup>3)</sup> Analytical and Testing Centre, Sichuan University, 610064, Chengdu, China

<sup>4)</sup> School of Physical Sciences, University of Kent, CT2 7NH, Canterbury, United Kingdom

(Dated: May 2017, <sup>+</sup> = these authors contributed equally to this work)

We report the observation of an unusual self-peeling effect which allows the synthesis of free standing vertically aligned carbon nanotubes films filled with large quantities of Fe<sub>3</sub>C and small quantities of  $\gamma$ -Fe crystals. We demonstrate that this effect depends on the interplay of three main factors: 1) the physical interactions between the chosen substrate surface and grown CNTs, which is fixed by the composition of the used substrate (111 SiO<sub>2</sub>/Si or quartz) 2) the CNT-CNT Van der Waals interactions and 3) the differential thermal contraction between the grown CNTs film and the used substrate, which is fixed by the cooling rate differences between the grown film and the used quartz or Si/SiO<sub>2</sub> substrates. The width and stability of these films is then further increased to cm-scale by addition of small quantities of toluene to the ferrocene precursor.

## Introduction

For more than a decade films of aligned multiwall carbon nanotubes (MWCNTs) filled with ferromagnetic  $\alpha$ -Fe and Fe<sub>3</sub>C have been an important subject of research owing to their attractive magnetic properties<sup>1-12</sup>.

These structures can indeed exhibit extremely large coercivities of 0.16-0.18 Tesla and high saturation magnetization values of 85 emu/g<sup>1, 4-10, 12</sup>. The magnetic tunability of these nanostructures was first demonstrated in 2005 when Leonhardt et al. reported a novel CVD approach for the synthesis of aligned MWCNTs films filled with a single phase of  $\alpha$ -Fe<sup>6</sup>. Further advancement in the synthesis of these filled-CNT structure films was achieved by Boi et al. in 2013 with the fabrication of MWCNTs-flower structures completely filled with  $\alpha$ -Fe<sup>7</sup>. Continuous  $\alpha$ -Fe filling was also reported recently in 2015 by Peci et al. for the case of vertically aligned CNT films grown with a temperature-gradient driven CVD method at low vapour flow rates<sup>20</sup>. Also in this case the use of additional annealing processes was considered<sup>20</sup>. The possibility of tuning the phase-composition of filled MWCNT-films without the use of annealing was demonstrated by Boi et al. via a flow-rate dependent CVD approach<sup>8</sup>.

Numerous research groups also reported the synthesis of large quantities of  $\alpha$ -Fe and Fe<sub>3</sub>C together with  $\gamma$ -Fe inside MWCNTs<sup>11-15</sup>, showing the possibility of applications such as magnetic data recording and exchange bias systems<sup>1, 12, 15, 16</sup>. Magnetic data recording and exchange bias are an important application for filled-MWCNT systems containing: 1) one ferromagnetic component in which the magnetic contribution is dominated by either

large uniaxial shape anisotropy<sup>6, 9, 10</sup> or/and large magnetocrystalline anisotropy<sup>12-14, 17</sup> or 2) one ferromagnetic component magnetically coupled with an antiferromagnetic component that induces a shift in the observed hysteresis loop (exchange bias)<sup>14-16</sup>.

In a typical magnetic data recording system, data densities higher than 66 Gigabit/inch<sup>2</sup> could be reached by recording one bit in each Fe-filled nanotube<sup>1</sup>. The high coercivities of these structures have been reported to depend strongly on crystal anisotropy, shape anisotropy, degree of alignment of the MWCNTs and exchange coupling or bias interactions<sup>6, 15, 16</sup>.

The synthesis of these films is generally performed by chemical vapour deposition (CVD) of an organometallic precursor known as ferrocene on the top of thermally oxidized Si/SiO<sub>2</sub> substrates<sup>1-19</sup>. Commonly used fabrication methods are solid-source CVD (SSCVD) and liquid-source CVD (LSCVD)<sup>19</sup>. The decomposed metallocene-vapour has been reported to contain Fe, H<sub>2</sub>, CH<sub>4</sub>, C<sub>5</sub>H<sub>6</sub> and other hydrocarbon species<sup>19</sup> that react on the substrate surface to form the metal particles from which the MWCNTs and single crystal filling will grow simultaneously. One of the major challenges in the growth of these nanostructures is the removal of the grown film from the used substrate without damaging the base of the MWCNTs and disrupting the high degree of alignment. In consideration of this, the recent work of Guo et al. has shown that the use of Cl-containing hydrocarbons can be beneficial for a better film stability through the control of the immediate CNT-CNT contact and thus the achievement of a higher number of Van der Waals interactions<sup>21</sup>.

In addition, the physical interactions between the grown CNTs and the used substrates can also play a key role in inducing a base-growth mechanism or a tip-growth mechanism of the CNTs<sup>19</sup>.

In this paper we report the observation of an unusual

<sup>a)</sup> Electronic mail: f.boi@scu.edu.cn

<sup>b)</sup> Electronic mail: m.willis@scu.edu.cn

<sup>c)</sup> Electronic mail: gxiang@scu.edu.cn

peeling-off effect which allows the direct self-detachment of vertically aligned CNTs filled with  $\text{Fe}_3\text{C}$  and  $\gamma\text{-Fe}$  from the substrate surface. We demonstrate that this effect depends on the interplay of three main factors: 1) the physical interactions between the chosen substrate and grown CNTs, which is fixed by the composition of the used substrate (111  $\text{SiO}_2/\text{Si}$  or quartz) 2) the Van der Waals interactions between each CNTs and 3) the differential thermal contraction between the grown CNTs film and the used substrate.

The stability of these films is then increased to reach sizes in the cm scale via the addition of small quantities of toluene to the ferrocene. The high alignment and high smoothness of the MWCNTs films together with the peeling-off mechanism are demonstrated through scanning electron microscopy (SEM). The filling rate is investigated through high resolution transmission electron microscopy (HRTEM). The phase composition is analysed through HRTEM and X-ray diffraction (XRD). The large coercivities of these structures (0.15 Tesla) are revealed by vibrating sample magnetometry (VSM) measurements and could be attributed to possible interactions of the  $\text{Fe}_3\text{C}$  phase with  $\gamma\text{-Fe}$ . The presence of unusual pinning-like steps in the hysteresis could be also a consequence of such interactions. However, magnetization reversal processes, involving domain wall nucleation processes, similar to those reported by Zhang et al.<sup>22</sup> can not be excluded.

### Experimental

Free-standing films of aligned MWCNTs filled with ferromagnetic  $\text{Fe}_3\text{C}$  were firstly produced by sublimation and pyrolysis of ferrocene (180 mg) inside a quartz tube-reactor of length 1.5 m at Ar flow rates of 11 ml/min (laminar flow). These structures were found across all the reactor inner-surface and on the used quartz substrates (thickness: 0.5-1 mm) placed inside.

The temperature of sublimation was approximately 300-350 °C. The formation of the free-standing films was achieved at a furnace temperature of 990 °C. The duration of each reaction was 20-25 minutes. The reactor was cooled to room temperature by sliding the furnace away along a rail system. In order to investigate the key role of the cooling rate in the MWCNTs film-detachment process, two sizes of quartz tubes were used: one with wall thickness of 2.5 mm (inner diameter 17 mm and outer diameter 22 mm) and another with a wall thickness of 1.5 mm (inner diameter 19 mm and outer diameter 22 mm).

In the case of the first tube-wall thickness a cooling rate of 50-70 °C per minute was achieved while in the case of the second tube-wall thickness a cooling rate of 100-140 °C per minute was achieved. In order to verify the presence of such a mechanism for thermally oxidized  $\text{Si}/\text{SiO}_2$  substrates, additional fabrication experiments were performed under similar conditions on the top of 111  $\text{Si}/\text{SiO}_2$  substrates using a CVD reactor with thickness of 2.5 mm.

The formation mechanism was also investigated at higher vapour flow rates of 100 and 150-180 ml/min.

The increase in the width of the MWCNTs-film to cm (large-scale) was then achieved by introducing toluene to ferrocene inside the first type of CVD system (wall thickness of 2.5 mm, inner diameter 17 mm and outer diameter 22 mm) by using a mixture of 180 mg of ferrocene and 2 drops (each drop is 0.05 ml) of toluene in the same synthesis conditions. The free-standing aligned MWCNTs films were magnetically removed (with a permanent magnet) from the reactor.

SEM investigations were performed with a JSM-7500F and an FEI Inspect F microscope at 15 and 20 kV. HRTEM investigations were performed using a 200 kV FEI Tecnai G2F20. XRD analyses were performed with a Philips Xpert pro MPD (Cu K- $\alpha$  source with  $\lambda = 0.154$  nm). The magnetic measurements were performed at room temperature by employing a VSM 2.5 Tesla electromagnet East Changing 9060 at the magnetic field of 1.3 Tesla.

### Results and Discussion

The morphology of the films obtained in the reaction performed in the first type of quartz tube reactors was shown by using SEM analyses. Typical examples of these films are presented in FIG. 1. Interestingly, the MWCNTs in these films demonstrate a very high alignment together with a high smoothness (FIG. 1(a)). The measured thickness of the free-standing MWCNTs films (approximately 20 micrometres) is highlighted in FIG. 1(a). Another example of these type of free-standing films is shown in Fig. Supp.1. In order to further investigate the role of the metallocene-concentration on this process, other experiments were performed at much higher flow rates of 100 and 150-180 ml/min. Curiously, these experiments revealed a disappearance of the MWCNTs self-peeling process at Ar flow rate values of 150-180 ml/min (see Figs. Supp. 7-10). This effect may suggest that the concentration of ferrocene vapour during the pyrolysis may affect the interactions between the growing film and the substrate surface leading to a different type of growth mechanism (i.e. base-growth mechanism instead of tip-growth mechanism).

We can therefore propose that the mechanism of formation of these structures consists of two steps: 1) nucleation and growth according with the nanotube growth mechanism described in the introduction<sup>19</sup> under conditions of very high ferrocene vapour concentration which leads to a weak interaction between CNTs and substrate and 2) peeling-off/detachment due to the fast-cooling rate. The cross-sectional morphology of a typical MWCNT in the free-standing films is shown in FIG. 1(b), while the single-crystalline properties of the encapsulated particles are shown by the yellow arrow in the inset. The HRTEM image (inset FIG. 1(b)) shows the typical 100 forbidden reflection of  $\text{Fe}_3\text{C}$  phase with space group  $\text{Pnma}$ <sup>23</sup> (see supplementary information Fig.2 for statistical plots of the particle diameter distribution).

These single-crystals were observed in more than 90% of the analyzed MWCNTs. In order to further investigate the role of differential thermal contraction on the peeling-

off process of the CNTs-films, additional experiments were performed using a thinner wall quartz tube reactor (the wall-thickness was decreased from 2.5 to 1.5 mm) to achieve a faster cooling rate of 100-140 °C per minute. As shown by FIG. 2, also in this case free-standing MWCNTs films with high alignment were found to detach from the quartz tube surface and from the quartz substrates surface (see FIG. 2(a,b)). However, in this case a lower film-thickness (5-10 micrometres) and a higher brittleness (see FIG. 2(a,b)) was found.

These findings confirm the dependence of the peeling-off process and film-stability on the differential thermal contraction effect induced by the different cooling rate of film and quartz-tube/substrate systems (see FIG. 3 for example of peeling-off-mechanism).

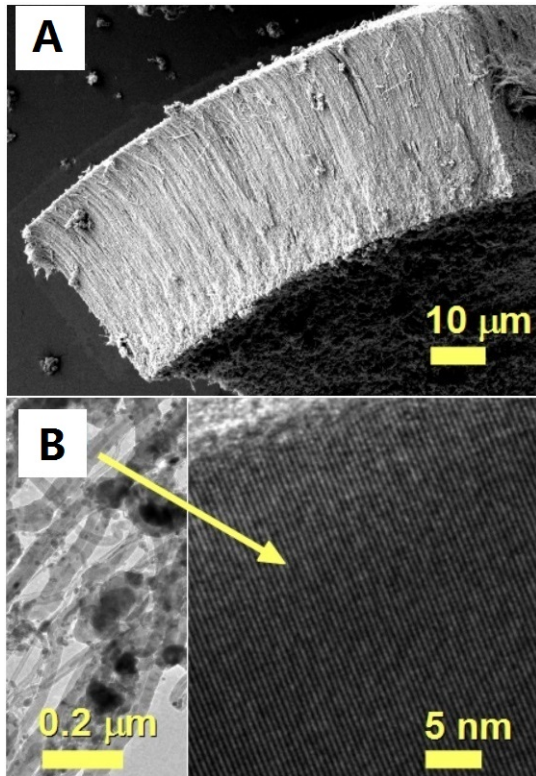


FIG. 1. Scanning electron micrograph showing in (a) the very high alignment of the filled carbon nanotubes comprised in the free-standing films. In (b) a transmission electron micrograph shows the cross-sectional morphology of the nanotubes, while the yellow arrow indicates the HRTEM micrograph of a typical  $\text{Fe}_3\text{C}$  single crystal exhibiting the kinematically (kinematical scattering selection rules) forbidden 100 reflection<sup>23</sup>.

It seems clear that the stability of the films increases with the increase of the length and closed-packing of the CNTs, thus it can be concluded that a key role is also played by the Van der Waals forces between each MWCNT. As to ascertain a deeper understanding of the role of the differential thermal contraction in such a peeling-off mechanism further experiments were performed using 111 Si/SiO<sub>2</sub> substrates with a thickness

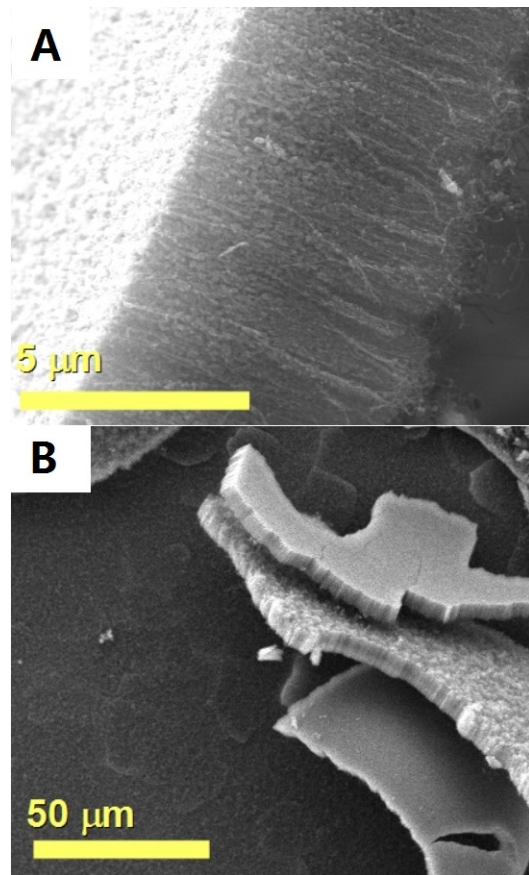


FIG. 2. Scanning electron micrographs showing in (a) the high alignment of the filled carbon nanotubes comprised in the free-standing films obtained with ferrocene-pyrolysis in quartz tube with wall-thickness of 1.5 mm. In (b) a top view of many free-standing films-flakes is shown.

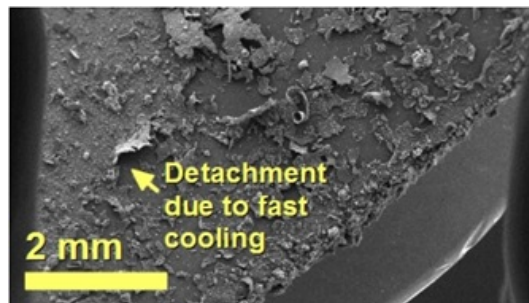


FIG. 3. SEM micrograph showing the detachment of the grown films from the quartz substrate surface due to the interplay of CNTs-substrate interactions and differential thermal contraction.

similar to that of the quartz substrates used in previous approaches (1 mm) (the other experimental conditions were equal to those used in the experimental section shown above for CVD reactor with wall thickness of 2.5 mm). The result of the experiments performed under these conditions is shown in Figs.3-5 Supp. Info.

Interestingly in these conditions the obtained films are

found to have a much larger width, in the order of many mm and a thickness in the order of 30 micrometres. These results confirm that a key factor in this peeling effect is the differential thermal contraction process. In addition it should be noted that a possible higher number of Van der Waals interactions may be present for long CNTs. Thus, the interplay of the local-cooling rate (differential thermal contraction), substrate-CNTs interactions and CNT-CNT physical interactions appear to be the key parameters in controlling this effect. With the aim of increasing the size of these structures, the introduction of a second carbon source in the CVD system with a quartz tube thickness of 2.5 mm and with same synthesis conditions, was considered (no substrate was used in this case).

Previous literature has shown that the addition of benzene-like hydrocarbons<sup>2,3</sup> can facilitate increasing of the size in empty aligned MWCNTs generally grown on Si/SiO<sub>2</sub> substrates. In this manner, 0.1 ml of toluene was added to 180 mg of ferrocene and pyrolysed in the same conditions described above. In this case no substrate was used. As shown in the image in the inset of FIG. 4(a) an increase in size is indeed observed with the width of the free-standing films increasing to 1.0-1.2 cm. The morphology of these films was also studied using SEM. The red arrow in FIG. 4(a) indicates a typical SEM micrograph, showing a top view of the cm-width of the film. Once again, a very high alignment (FIG. 4(b)) of the nanotubes was found together with a very high mechanical stability (i.e. the films were easily transferable with tweezers without damage). The phase composition of the cm-size films was then investigated with XRD (see supplementary information Fig. 6). The Rietveld refinement revealed a large quantity of Fe<sub>3</sub>C (93%) together with a small quantity of  $\gamma$ -Fe (7%) which can be attributed to the pressure imposed by the MWCNTs walls.

The magnetic properties of the cm-size free standing films were then investigated using VSM. FIG. 5 shows a typical hysteresis loop obtained from a single cm-size film of filled MWCNTs. A large coercive-force of 0.15 Tesla and a saturation magnetization of 12 emu/g were measured. The saturation magnetization is much lower with respect to that expected for bulk Fe<sub>3</sub>C (169 emu/g) and can be attributed to the low filling rate of the MWCNTs. In contrast, the coercive force is much larger with respect to the coercivities of polycrystalline Fe (0.0001 Tesla) and Fe (0.0023 Tesla)<sup>14</sup>. In fact, the coercivity is also much higher than those measured at room temperature by Prados et al. (0.08 Tesla)<sup>15</sup>, Karmakar et al. (0.066 Tesla)<sup>14</sup>, Aaron Morelos-Gomez et al. (0.08 Tesla)<sup>12</sup> and Lv et al. (0.05 Tesla)<sup>14</sup> but slightly lower than that measured by Hampel et al (0.180 Tesla)<sup>9</sup> for the case of surface-grown MWCNTs filled with mixed Fe-phases.

This difference in the result of Hampel et al. is owing to the different shape anisotropy contribution. In this case, a possible influence of the  $\gamma$ -Fe on the measured coercivity also cannot be excluded. Recent work

has indeed shown that the presence of  $\gamma$ -Fe can lead to unusual magnetic arrangement of MWCNTs films and to increases in the coercivity<sup>14-16</sup>. This extremely large value of the coercivity makes the free-standing MWCNTs films suitable candidates as electrodes for capacitor applications, where high surface areas, high smoothness and large coercive-force are required. The presence of unusual step features in FIG. 5 could be also considered a consequence of possible Fe<sub>3</sub>C/  $\gamma$ -Fe interactions. However, the possible presence of magnetization reversal behaviors involving the nucleation and propagation of domain walls can not be excluded<sup>22</sup>.

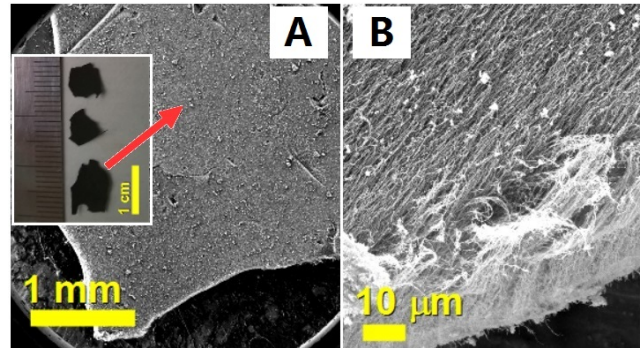


FIG. 4. Scanning electron micrographs (a-b) showing with a top view the morphology of the cm-size free-standing filled carbon nanotube films obtained with pyrolysis of ferrocene-toluene mixtures. In the inset in (a) a photograph showing the cm width of the MWCNTs film is shown. The high alignment of the MWCNTs comprised in the cm-size film is shown in the micrograph in b. In some regions of the films the MWCNTs alignment was slightly damaged by the pressure required for the SEM-sample mounting-procedure.

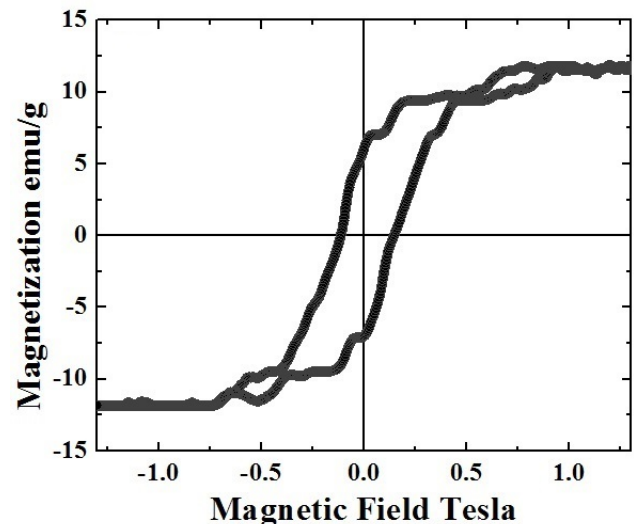


FIG. 5. Typical room temperature hysteresis loop (sat. magnetization of 12 emu/g) of a single cm-width film of aligned MWCNTs filled with Fe<sub>3</sub>C and  $\gamma$ -Fe.



## Conclusions

In conclusion we reported the observation of an unusual peeling-off effect of vertically aligned CNTs filled  $\text{Fe}_3\text{C}$  and  $\gamma\text{-Fe}$ . We demonstrated that this effect depends on the interplay of three main factors: 1) the physical interactions between the chosen substrate and grown CNTs 2) the Van der Waals interactions between the CNTs in the film 3) the differential thermal contraction between the grown CNTs film and the used substrate. The mechanical stability of these films was then increased to reach sizes in cm scale by addition of small quantities of toluene to ferrocene. The properties of the films have been investigated in detail with SEM, TEM and XRD as well as VSM for the mixed source case.

## Supplementary Material

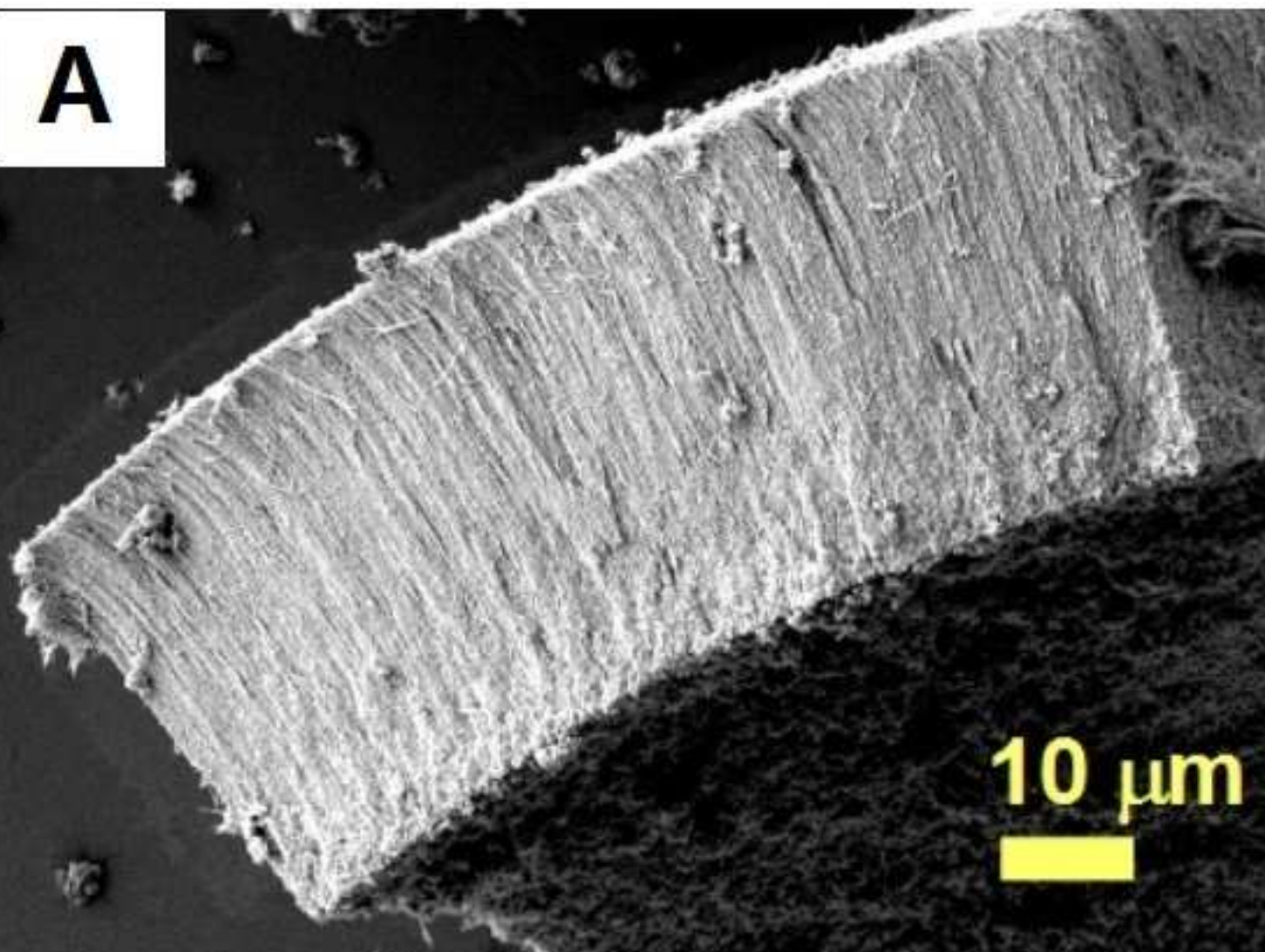
See supplementary material [URL will be inserted by AIP] for additional micrographs showing the peeling off mechanism and additional structural XRD analyses

## I. ACKNOWLEDGMENTS

We acknowledge Prof. Gong Min for his continuous support and the National Natural Science Foundation of China Grant No 11404227. We also acknowledge Mark Baxendale for helpful discussion.

## II. REFERENCES

- <sup>1</sup>H. Terrones, F. Lopez-Urias, E. Munoz-Sandoval, J. A. Rodriguez-Manzo, A. Zamudio, A.L. Elias and M. Terrones . *Solid State Sciences*, **8** 303,(2006).
- <sup>2</sup>S. S. Meysami, F. Dillon, A. A. Koos, Z. Aslam, N. Grobert. *Carbon*, **58** 151,(2013).
- <sup>3</sup>S. S. Meysami, A. A. Koos, F. Dillon, N. Grobert. *Carbon*, **58** 159,(2013).
- <sup>4</sup>A. L. Danilyuk, A. L. Prudnikava, I. V. Komissarov, K. I. Yanushkevich, A. Derory, F. Le Normand, V. A. Labunov, S. L. Prischepa. *Carbon*, **68** 337,(2014).
- <sup>5</sup>F. C. Dillon, A. Bajpai, A. Koos, S. Downes, Z. Aslam and N. Grobert. *Carbon*, **50** 3674,(2012).
- <sup>6</sup>A. Leonhardt, M. Ritschel, M.; Elefant, D. N. Mattern, K. Biedermann, S. Hampel, Ch. Muller, T. Gemming, B. Buchner. *Journal of Applied Physics*, **98** 074315,(2005).
- <sup>7</sup>F. S. Boi, G. Mountjoy, R. M. Wilson, Z. Luklinska, L. J. Sawiak, M. Baxendale. *Carbon*, **64** 351,(2013).
- <sup>8</sup>F. S. Boi, S. Maugeri, J. Guo, M. Lan, S. Wang, J. Wen, G. Mountjoy, M. Baxendale G. Nevill, R. M. Wilson, Y. He, S. Zhang, G. Xiang. *Appl. Phys. Lett.*, **105** 243108,(2014).
- <sup>9</sup>S. Hampel, A. Leonhardt, D. Selbmann, K Biedermann, D. Elefant, Ch. Muller, T. Gemming and B. Buchner. *Carbon*, **44** 2316,(2006).
- <sup>10</sup>C. Muller, S. Hampel, D. Elefant, K. Biedermann, A. Leonhardt, M. Ritschel, B. Buchner. *Carbon*, **44** 1746,(2006).
- <sup>11</sup>A. Leonhardt, M. Ritschel, R. Kozhuharova, A. Graffa, T. Muhl, R. Huhle, I. Monch, D. Elefant and C.M. Schneider. *Diamond and Related Materials*, **12** 790,(2003).
- <sup>12</sup>A. Morelos-Gomez, F. Lopez-Urias, E. Munoz-Sandoval, C. L. Dennis, R. D. Shull, H. Terrones and M. Terrones. *Journal of Material Chemistry*, **20** 5906,(2010).
- <sup>13</sup>D. Golberg, M. Mitome, Ch. Muller, C. Tang, A. Leonhardt, Y. Bando. *Acta Materialia*, **54** 2567,(2006).
- <sup>14</sup>S. Karmakar, S. M. Sharma, M. D. Mukadam, S. M. Yusuf and A. K. Sood. *Journal of Applied Physics*, **97** 054306,(2005).
- <sup>15</sup>C. Prados, P. Crespo, J. M. Gonzalez, A. Hernando, J. F. Marco, R. Gancedo, N. Grobert, M. Terrones, R. M. Walton and H. W. Kroto. *Physical Review B*, **65** 113405,(2002).
- <sup>16</sup>J. F. Marco, J. R. Gancedo, A. Hernando, P. Crespo, C. Prados, J. M. Gonzalez, N. Grobert, M. Terrones, D. R. M. Walton and H. W. Kroto. *Hyperfine Interactions*, **139** 535,(2002).
- <sup>17</sup>R. Lv, S. Tsuge, X. Gui, K. Takai, F. Kang, T. Enoki, J. Wei, J. Gu, K. Wang and D. Wu. *Carbon*, **47** 1141,(2009).
- <sup>18</sup>C. Muller, D. Golberg, A. Leonhardt, S. Hampel, B. Buchner. *Physica status solidi (a)*, **6** 1064,(2006).
- <sup>19</sup>U. Weissker, S. Hampel, A. Leonhardt and B. Buchner. *Materials*, **3** 4387,(2010).
- <sup>20</sup>T. Peci, M. Baxendale. *Carbon*, **98** 519-525,(2015).
- <sup>21</sup>J. Guo, Y. He, S. Wang and F. S. Boi. *Carbon*, **102** 372-82,(2016).
- <sup>22</sup>W. Zhang, M. E. Bowden, K. M. Krishnan. *Journal of Applied Physics*, **113** 17B502,(2013).
- <sup>23</sup>F. S. Boi, G. Mountjoy, Z. Luklinska, L. Spillane, L. S. Karlsson, R. M. Wilson, A. Corrias and M. Baxendale. *Microscopy and Microanalysis*, **19** 1298,(2013).

**A****B**

Transmission electron micrograph (TEM) showing a cross-section of a layered material. The image displays a complex, irregular structure with various shades of gray. A yellow scale bar in the bottom left corner indicates a length of  $0.2\ \mu\text{m}$ .

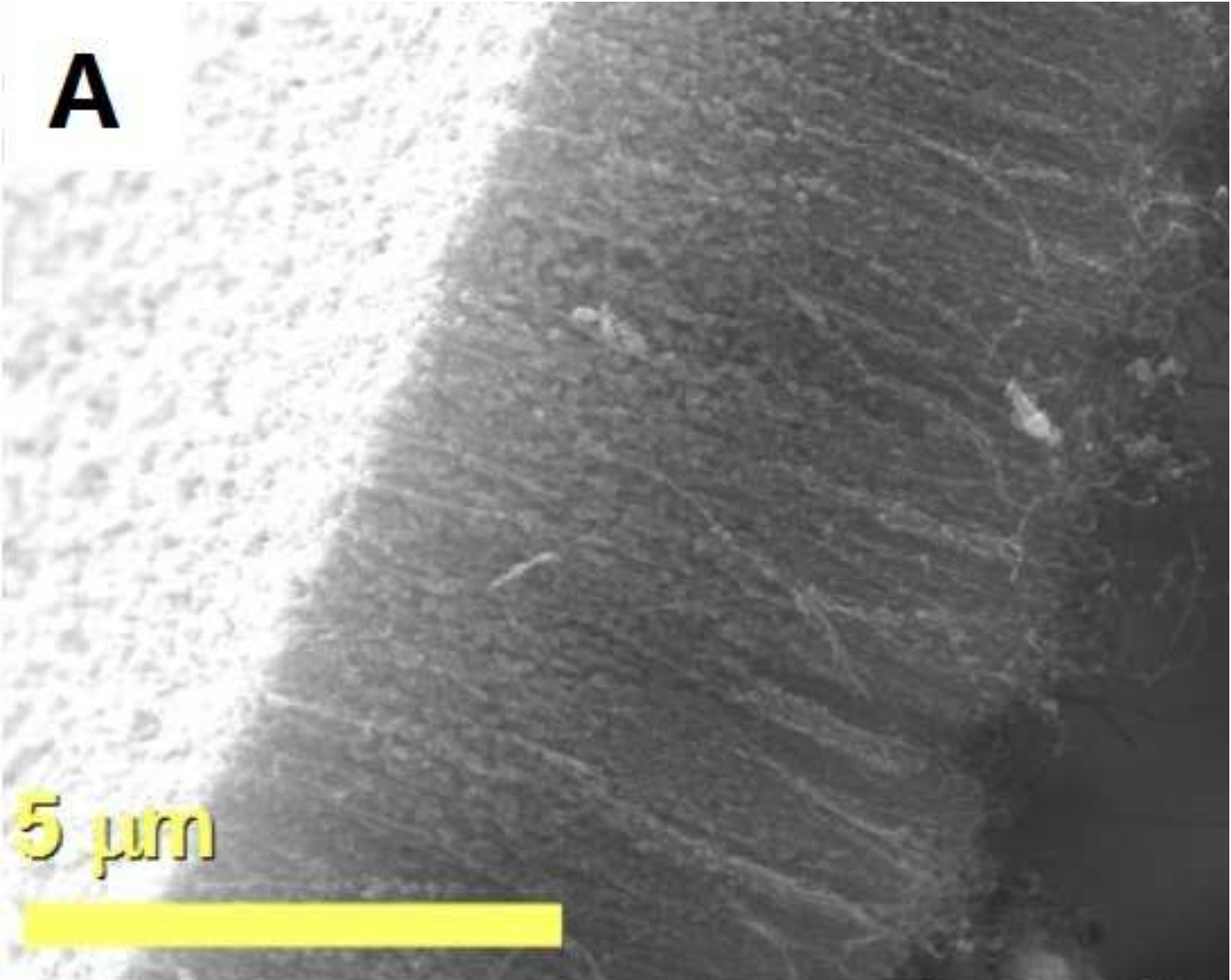
$0.2\ \mu\text{m}$

High-resolution transmission electron micrograph (HRTEM) showing a cross-section of a layered material. The image displays a highly ordered, periodic structure with a clear lattice pattern. A yellow arrow from the TEM image above points to this HRTEM image. A yellow scale bar in the bottom right corner indicates a length of  $5\ \text{nm}$ .

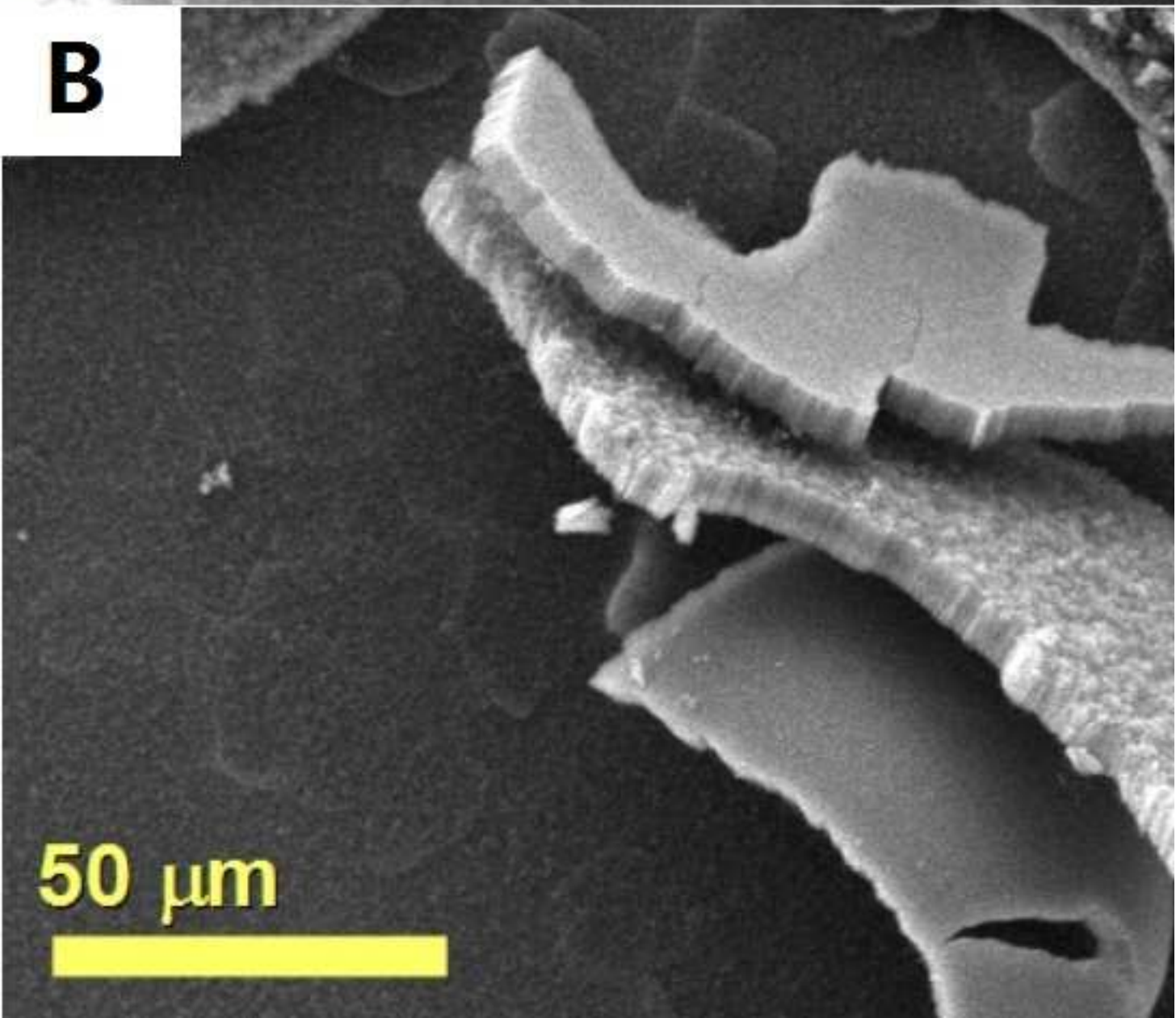
$5\ \text{nm}$

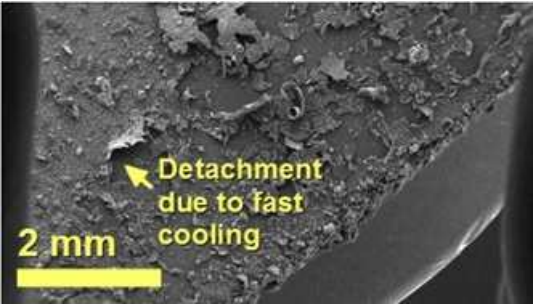


**A**



**B**



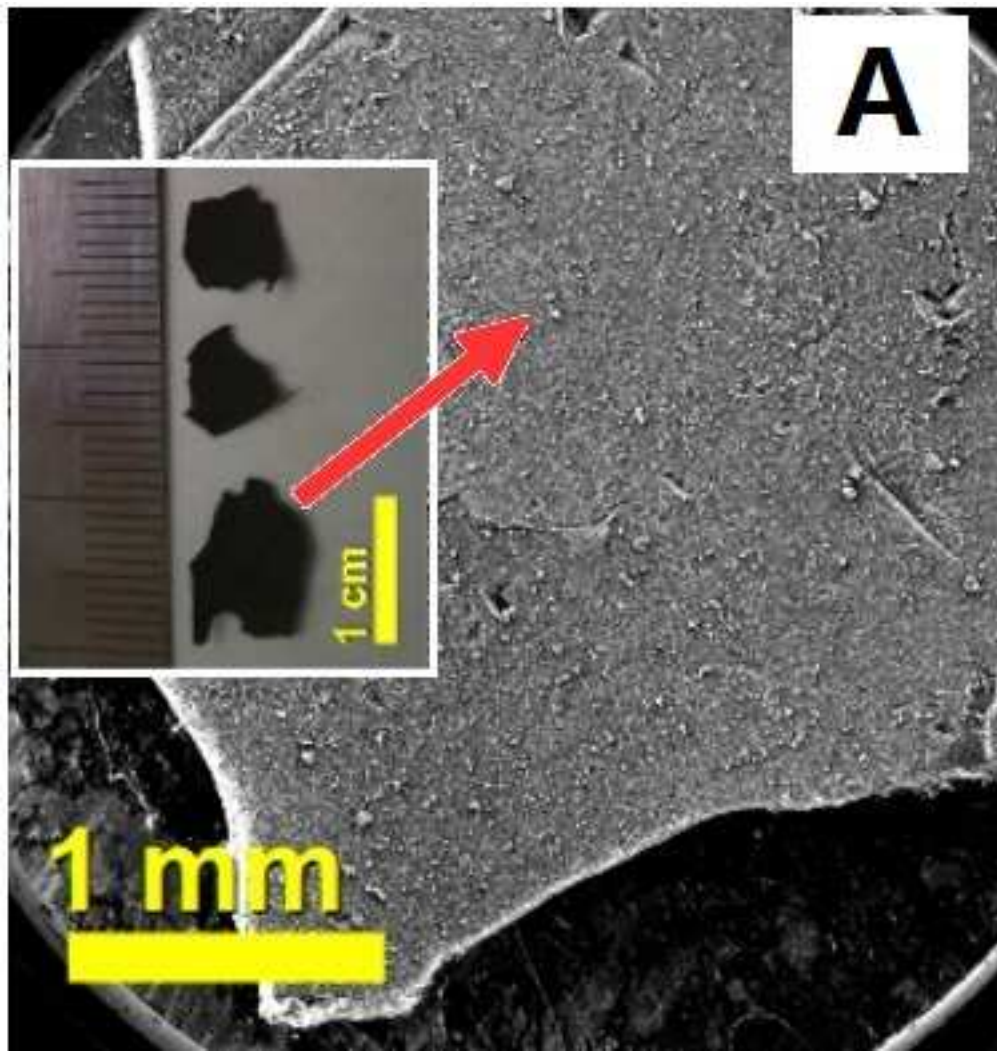
Scanning electron micrograph (SEM) showing a textured surface. A yellow arrow points to a specific area of surface detachment. The surface has a granular, porous appearance with various sized particles and irregular shapes. A dark, curved feature is visible in the lower right corner.

**Detachment  
due to fast  
cooling**

**2 mm**





**A****B**